iScience

CellPress
OPEN ACCESS

Article

Glioblastoma stem cell-derived exosomal miR-374b-3p promotes tumor angiogenesis and progression through inducing M2 macrophages polarization

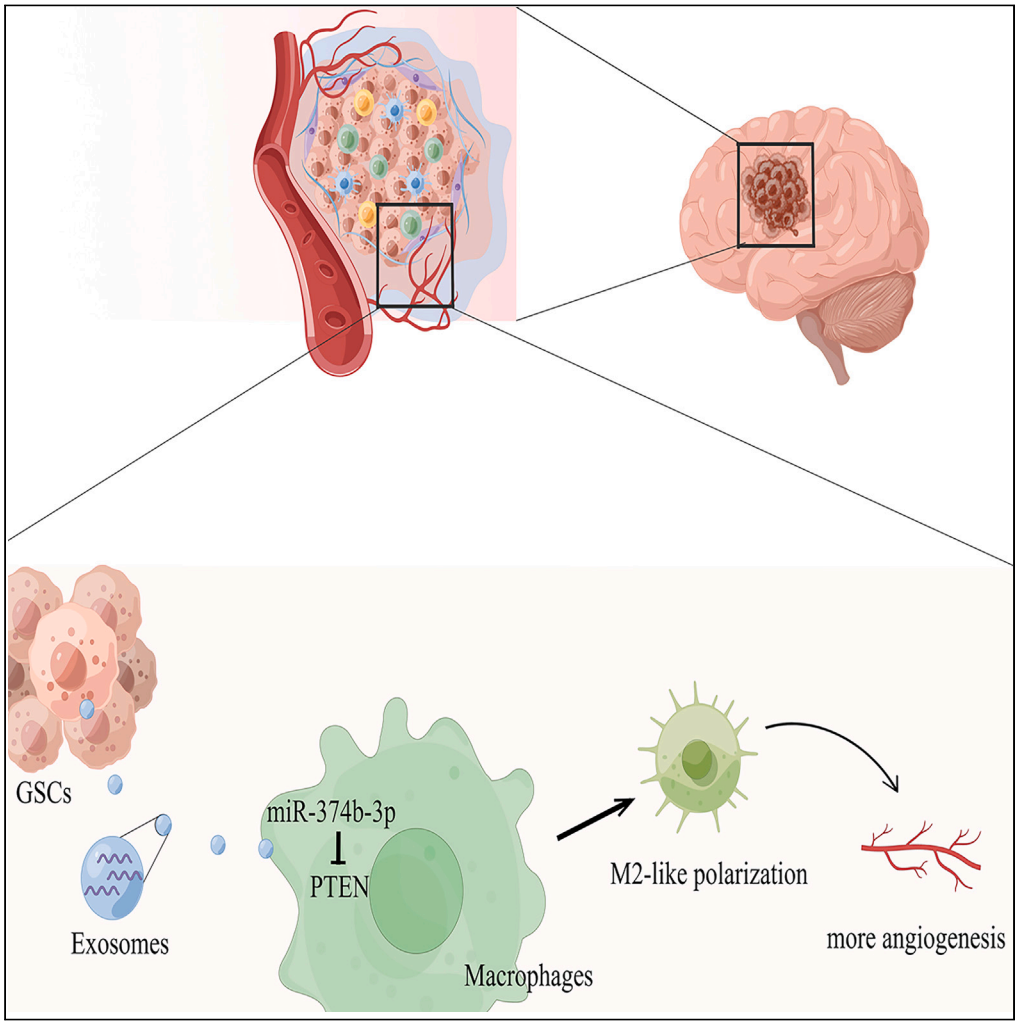

Shilu Huang, Peng Zhang, Nanheng Yin, ..., Liang Liu, Yan Shi, Jun Dong

dongjun@suda.edu.cn

Highlights

The miR-374b-3p was increased in clinical glioblastoma specimens, GSCs and GSCs-exos

GSCs-exos promoted glioblastoma angiogenesis through M2 polarization of macrophages

GSCs exosomal miR-374b-3p induced M2 polarization of macrophages by regulating PTEN

Huang et al., iScience 27, 109270
March 15, 2024
https://doi.org/10.1016/j.isci.2024.109270

iScience

CellPress
OPEN ACCESS

Article

Glioblastoma stem cell-derived exosomal miR-374b-3p promotes tumor angiogenesis and progression through inducing M2 macrophages polarization

Shilu Huang,[1,4] Peng Zhang,[2,4] Nanheng Yin,[1] Zhipeng Xu,[1] Xinglei Liu,[1] Anyi Wu,[1] Xiaopei Zhang,[1] Zengyang Li,[1] Zhicheng Zhang,[1] Tao Zhong,[1] Liang Liu,[3] Yan Shi,[1] and Jun Dong[1,5,*]

SUMMARY

Glioblastoma stem cells (GSCs) reside in hypoxic periarteriolar niches of glioblastoma micro-environment, however, the crosstalk of GSCs with macrophages on regulating tumor angiogenesis and progression are not fully elucidated. GSCs-derived exosomes (GSCs-exos) are essential mediators during tumor immune-microenvironment remodeling initiated by GSCs, resulting in M2 polarization of tumor-associated macrophages (TAMs) as we reported previously. Our data disclosed aberrant upregulation of miR-374b-3p in both clinical glioblastoma specimens and human cell lines of GSCs. MiR-374b-3p level was high in GSCs-exos and can be internalized by macrophages. Mechanistically, GSCs exosomal miR-374b-3p induced M2 polarization of macrophages by downregulating phosphatase and tensin expression, thereby promoting migration and tube formation of vascular endothelial cells after coculture with M2 macrophages. Cumulatively, these data indicated that GSCs exosomal miR-374b-3p can enhance tumor angiogenesis by inducing M2 polarization of macrophages, as well as promote malignant progression of glioblastoma. Targeting exosomal miR-374b-3p may serve as a potential target against glioblastoma.

INTRODUCTION

Glioblastoma is one of the most common and lethal primary brain malignancies in adults.[1] The median over survival of diagnosed patients is less than 15 months, even under the current standard comprehensive treatments.[2] Glioblastoma displays striking cellular heterogeneity and hierarchy, glioblastoma stem cells (GSCs) at the apex of this hierarchy contribute to treatment resistance and tissue remodeling resulting in tumor recurrence.[3,4] Although it was widely known that glioblastoma cells, especially the GSCs, play a vital role in promoting tumor angiogenesis directly,[5,6] increasing studies have confirmed that tumor immune-microenvironment (TIME) play active roles on inducing chemotaxis, proliferation, and migration of vascular endothelial cells, thus contributing to construction of tumor vasculature.[7]

Glioblastoma TIME is mainly dominated by immunosuppressive tumor-associated macrophages (TAMs) that limit immune surveillance and anti-tumor immunity.[8] A close association between TAMs and poor prognosis has been confirmed in various cancers including glioblastoma.[9] TAMs can be converted into different phenotypes in response to dynamically changing tumor microenvironment, classified as tumor suppressive (M1 type) or tumour-supportive (M2 type) macrophages.[10–12] Both TAMs and GSCs are localized, maintained in tumor perivascular niches.[13] TAMs can secrete certain pro-angiogenic cytokines, growth factors, and angiogenic regulatory enzymes to trigger angiogenic switch for construction of glioblastoma vasculature, thus promoting tumor development.[14] However, the mechanisms of GSCs remodeling the phenotypes of macrophages into anti-inflammatory and pro-tumor angiogenesis M2 type have not been fully elucidated.

Exosomes, as extracellular membrane vesicles approximately 30–150 nm in diameter, have been shown to be involved in regulating development of many malignancies.[15,16] Exosomes contain proteins, dsDNA, mRNAs, and non-coding RNAs, which can act as messenger between intercellular crosstalk in TIME.[17,18] Exosomal miRNAs from tumor cells have been found to regulate essential aspects of cancer, including angiogenesis, immunosuppression, and metastasis by remodeling the phenotype and function of recipient cells in TIME.[19] However, the roles of GSCs exosomal miRNAs on polarization of TAMs to enhance angiogenesis thus promoting glioblastoma progression deserve further investigations.

[1]Department of Neurosurgery, The Second Affiliated Hospital of Soochow University, Suzhou 215004, China
[2]Department of Neurosurgery, Rugao People's Hospital, RuGao 226500, China
[3]Department of Neurosurgery, Affiliated Nanjing Brain Hospital, Nanjing Medical University, Nanjing, China
[4]These authors contributed equally
[5]Lead contact
*Correspondence: dongjun@suda.edu.cn
https://doi.org/10.1016/j.isci.2024.109270

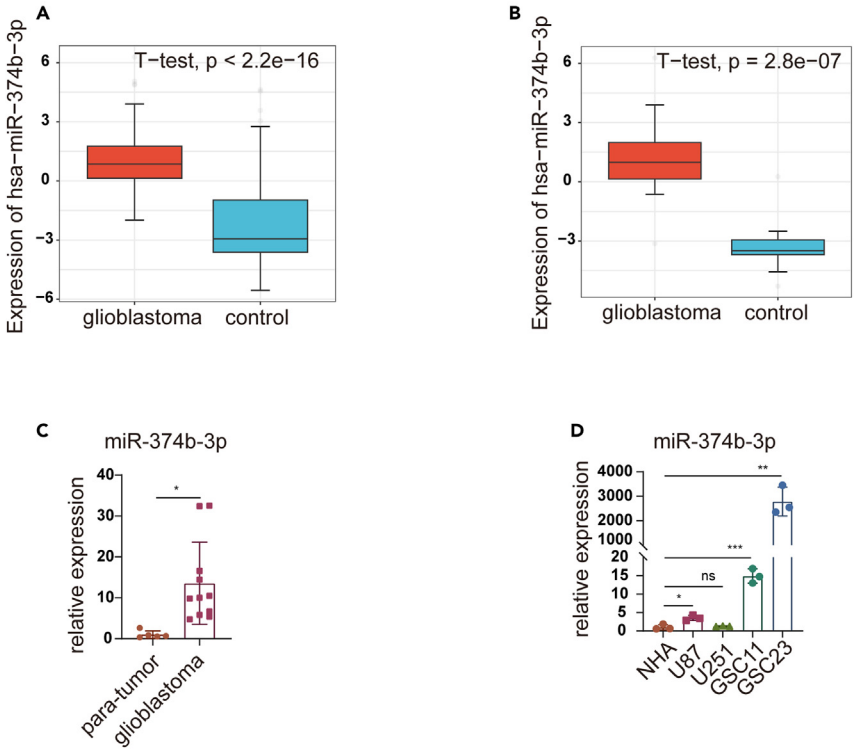

Figure 1. Aberrant expression of miR-374b-3p significantly correlated with glioblastoma patients

(A and B) Expression levels of miR-374b-3p in serum of two miRNA-seq datasets from the GEO database (https://www.ncbi.nlm.nih.gov/geo/) classified on the basis of glioblastoma patients and healthy control.

(C) The expression levels of miR-374b-3p in para-tumor tissue and glioma tissues were determined by RT-qPCR.

(D) The expression level of miR-374b-3p in GSCs (GSC11 and GSC23), glioblastoma cell lines (U87 and U251) and astrocytes (NHAs) were determined by RT-qPCR. Data are represented as means ± SD. Statistical analysis of the data from two groups was performed using Student's *t* test. (*p < 0.05; **p < 0.01; ***p < 0.001, ns: no significance).

To elucidate the regulatory mechanisms underlying GSCs exosomal miRNAs in upregulating glioblastoma angiogenesis, profiling of GSCs exosomal miRNAs[20] disclosed the expression pattern of miR-374b-3p was associated with tumor vascular, hence the roles of GSCs exosomal miR-374b-3p on promoting glioblastoma angiogenesis and progression were investigated for the purpose of identifying a useful biomarker and developing therapeutic strategies against glioblastoma angiogenesis.

RESULTS

MiR-374b-3p is upregulated in glioblastoma and GSCs, as well as rich in GSCs-exos

Expression status of miR-374b-3p in glioblastoma was evaluated through online bioinformatic analysis on expression profiles of miR-374b-3p in serum of glioblastoma patients and healthy donors, based on latest two miRNA-seq datasets from Gene Expression Omnibus database (GEO). GSE139031 and GSE113740, which disclosed that the expression of miR-374b-3p was significantly higher in serum of glioblastoma patients than that in healthy donors (Figures 1A and 1B). Besides, miR-374b-3p level elevated obviously in glioblastoma tissue, compared with peri-tumor tissue (Figure 1C), and miR-374b-3p level was high in GSCs (GSC11 and GSC23) than in normal human astrocytes (NHAs) and glioblastoma cell lines (U87 and U251), verified by RT-qPCR (Figure 1D), indicating that aberrantly high expression of miR-374b-3p was associated with glioblastoma and GSCs.

GSC-exos promote glioblastoma development

The exosomes from GSCs or NHAs were isolated by ultracentrifugation. Transmission electron microscopy (TEM) verified that the harvested exosomes were vesicle-like structures with size ranged from 30 to 150 nm (Figure 2A). Particle size analysis of the exosomes further confirmed that these particles distributed mainly varied in 30–150 nm (Figure 2B), which contained their specific markers (HSP70 and CD9) but negative for endoplasmic reticulum marker Calnexin (Figure S1). To investigate the role of GSC-exos in glioblastoma, SNB19 cells were implanted *in situ* in the right caudate nucleus of BALB/c nude mice, then NHA-exos or GSC23-exos were injected intravenously through tail vein in tumor-bearing mice. After five weeks, mice were sacrificed, their entire brains were harvested and brain slices were prepared, HE staining showed

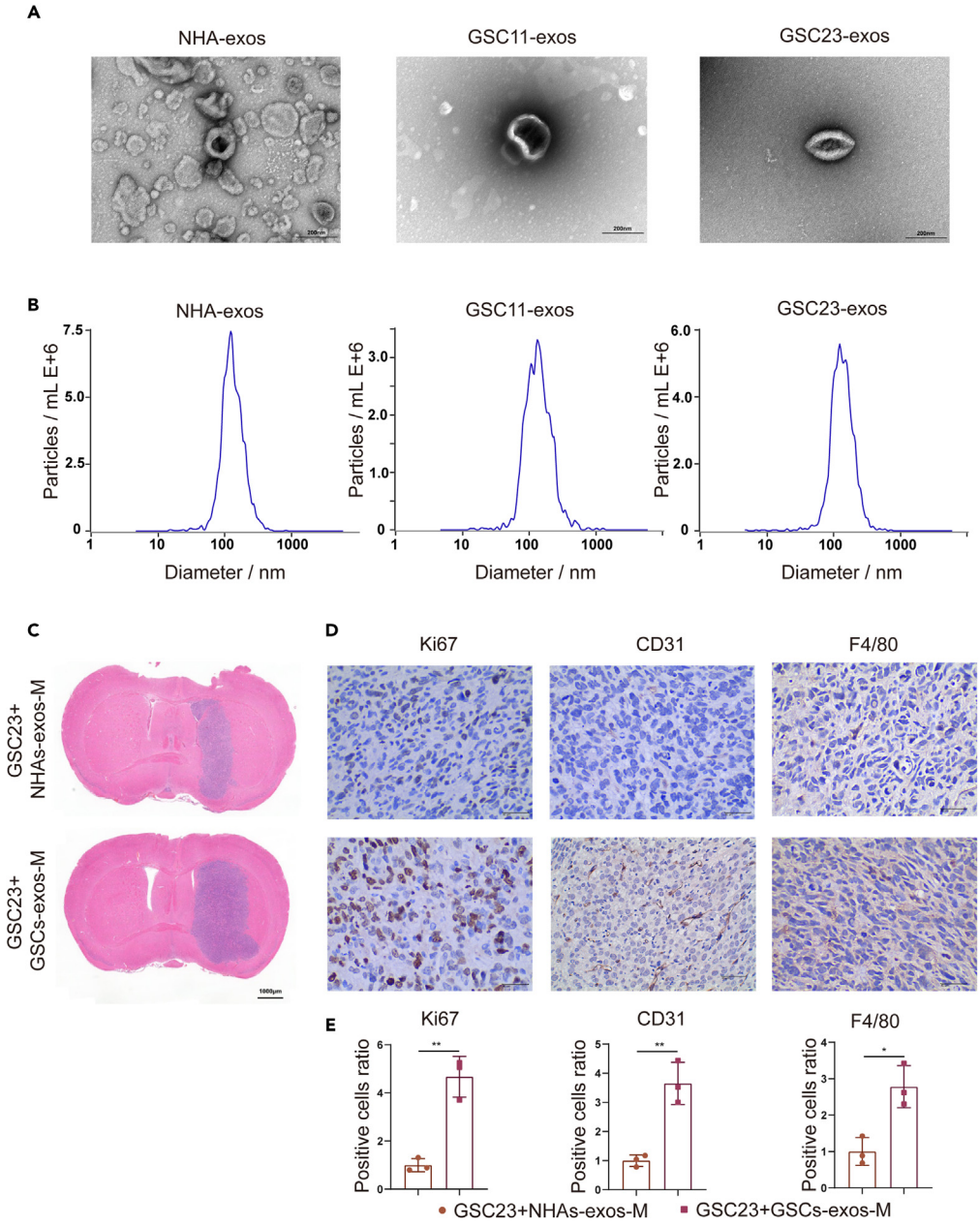

Figure 2. GSC-exos promoted glioblastoma development

(A) Representative transmission electron microscopy images of exosomes from NHAs, GSC11, and GSC23 cells, respectively (scale bar, 200 nm).

(B) Nanoparticle tracking the size distribution of exosomes from NHAs, GSC11, and GSC23 cells.

(C) *In vivo* evaluation of tumorigenesis in orthotopic xenograft nude mice bearing $5X10^5$ SNB19 cells inoculation with tail vein injection of 100 μL NHAs-exos or GSC23-exos. Representative intracranial tumor xenografts of HE staining images are shown (scale bar, 1000 μm).

(D and E) Representative images and quantification of IHC staining for Ki67, F4/80 and CD31 in sections from the intracranial SNB19 xenografts, indicating intratumoral upregulation of the three marker in GSC23-exos group (scale bar, 40 μm). Data are represented as means ± SD. Statistical analysis of the data from two groups was performed using Student's *t* test. (*$p < 0.05$; **$p < 0.01$).

that GSC23-exos significantly increased intracranial tumors growth, compared with the NHA-exos group (Figure 2C). Furthermore, immunohistochemical staining revealed that intravenous injection of GSC23-exos resulted in enhanced glioblastoma cells proliferation with increased number of $Ki67^+$ cells in tumor sections of xenografts. Macrophages infiltration was evaluated by counting $F4/80^+$ macrophages, which disclosed that the amount of $F4/80^+$ macrophages in xenografts was more in GSC23-exos group ($p < 0.05$). Disorganized dense blood vessels determined by counting $CD31^+$ blood vessels within intracerebral tumor sections showed increased angiogenesis in GSC23-exos group

($p < 0.01$) (Figures 2D and 2E). These results indicated that GSC23-exos promoted glioblastoma development via enhancing tumor cell proliferation, macrophages infiltration as well as upregulation of angiogenesis by GSCs exosomal miR-374b-3p induced macrophages.

GSCs exosomal miR-374b-3p promotes macrophages M2 polarization

RT-qPCR showed that the expression level of miR-374b-3p in exosomes derived from both GSC11 and GSC23 cells was higher than that of NHAs-exos (Figure 3A). Human THP-1 monocytes treated with 12-myristate-13-acetate (PMA) for 24–48 h to induce differentiation into macrophages. To evaluate whether macrophages can engulf exosomes derived from NHAs or GSCs, PKH26 (red fluorescence)-labeled exosomes were cocultured with macrophages, which disclosed that DAPI-labeled macrophages internalized the PKH26-labeled exosomes under confocal microscopic observation (Figure S2). Higher expression of miR-374b-3p can be detected in macrophages incubated with GSCs-exos by RT-qPCR, which was elevated higher than macrophages incubated either with NHAs-exos, or PBS only (Figure 3B). To investigate the role of GSCs exosomal miR-374b-3p on polarization of macrophages, macrophages were transfected with miR-374b-3p mimics or cocultured with GSC-exos, RT-qPCR was performed to evaluate macrophages markers expression, which showed that the expression of M2 markers (CD163, Arg1) increased, M1 marker CD80 decreased, another M1 marker iNOS kept in no obvious changes in macrophages after transfected with miR-374b-3p mimics (Figure 3C). Besides, macrophages coculturing with GSC11-exos or GSC23-exos resulted upregulation of M2 markers (CD163, Arg1) expression, which increased significantly, no obvious expression changes of M1 markers (CD80 and iNOS) can be detected in THP-1 cell-derived macrophages. Furthermore, transfection with miR-374b-3p inhibitor decreased M2 markers expression (Figures 3D and 3E). ELISA results showed that transfection of miR-374b-3p mimics promoted the IL-10 secretion of macrophages and inhibited the TNF-α secretion (Figures 3F and 3G). Flow cytometry showed that the proportion of $CD11b^{+}CD163^{+}$ double-positive macrophages increased after miR-374b-3p mimics transfection either THP-1 cells derived or healthy adult PBMCs-derived macrophages (Figures 3H, 3I, and S3), the proportion of $CD11b^{+}CD163^{+}$ double-positive macrophages increased after coculturing with GSCs-exos, $CD11b^{+}CD163^{+}$ macrophages decreased after transfection with miR-374b-3p inhibitors (Figure 3J). The gating strategies from representative plots are shown in S4. These results indicated that GSCs exosomal miR-374b-3p can induce M2 polarization of macrophages.

GSCs exosomal miR-374b-3p promote tumori-angiogenesis by inducing M2 polarization of macrophages

M2 polarization of macrophages has been reported to directly influence tumor cell survival, growth, and metastasis by promoting tumor angiogenesis.[21,22] In addition, MMP9 and TGF-β secreted by M2 macrophages have been shown to be involved in tumor angiogenesis.[23,24] After coculturing with miR-374b-3p mimics or GSCs-exos, the supernatant of macrophages culture medium was assayed with ELISA, which disclosed significantly increased vascular-associated cytokines (MMP9 and TGF-β) secretion by macrophages compared with those of macrophages coculturing with PBS, NHAs-exos, or NC mimics (Figures 4A and 4B). Subsequently, the indirect *in vitro* coculture system were further applied to investigate the role of miR-374b-3p mimics and GSCs-exos treated macrophages in promoting glioblastoma angiogenesis, wound-healing assays and transwell assays indicated that coculture with M2 macrophages induced by addition of GSCs-exos significantly increased the migration of endothelial cells Human umbilical vein endothelial cells (HUVECs) than addition of NHA-exos and PBS, and M2 macrophages induced by transfection of miR-374b-3p mimics significantly increased the migration of endothelial cells HUVECs than transfection of NC mimics (Figures 4C–4F; S5). Tube formation assay was then performed to detect whether macrophages polarized by GSCs-exos or miR-374b-3p mimics affect angiogenesis. When cocultured with M2 macrophages either induced by addition of GSCs-exos or miR-374b-3p mimics transfection, the branches of micro-tubules formed by endothelial cells HUVECs increased significantly (Figures 4G–4I). Collectively, GSCs exosomal miR-374b-3p promotes angiogenesis via polarized M2 macrophages.

PTEN is the functional target of GSCs exosomal miR-374b-3p in macrophages

The pro-angiogenesis regulatory pathway of M2 macrophage polarization by GSCs-derived exosomal miR-374b-3p was further explored. Bioinformatic prediction with TargetScan Human 7.2 database was performed, which disclosed that there was an alignment between the miR-374b-3p sequence and the 3′UTR sequence of phosphatase and tensin homolog (PTEN) (Figure 5A), suggesting the possibility of miR-374b-3p targeting PTEN on regulating M2 macrophage polarization. Previous studies have shown that PTEN was involved in macrophage polarization in cancer.[25] Then dual-luciferase assay was conducted, which showed that luciferase activity in 293T cells was significantly attenuated when co-transfected with Luc-PTEN-3′UTR-WT and miR-374b-3p mimics, whereas no change was observed when co-transfected with Luc-PTEN-3′UTR-MUT and miR-374b-3p mimics (Figure 5B), suggesting that miR-374b-3p directly targets PTEN. In addition, lower PTEN expression can be observed in glioblastoma tissue than in peri-tumor tissue (Figure 5C). After transfection of the mimics or inhibitors of miR-374b-3p into macrophages, PTEN expression was downregulated or upregulated, respectively (Figure 5D). Similarly, supplementation of GSCs-exos decreased PTEN expression in macrophages, while knockdown of miR-374b-3p increased PTEN expression (Figure 5E). The effect of PTEN overexpression in macrophages can be partially attenuated by transfection of miR-374b-3p mimics (Figure 5F). The effect of upregulation of M2 markers expression by miR-374b-3p mimics transfection can be diminished after co-transfection with PTEN over-expression plasmid, verified by RT-qPCR and flow cytometry analysis, respectively. (Figures 5G and 5H).

To explore the function of PTEN expression in macrophages on regulating angiogenic ability of endothelial cells, knockdown of PTEN with small interfering RNAs was conducted in THP-1 derived macrophages, knockdown efficiency in macrophages was verified by western blot (Figure 6A). Knockdown of PTEN significantly increased the expression of M2 markers (CD163 and Arg1), while no effect on M1 markers (CD80 and iNOS) expression, verified by RT-qPCR (Figure 6B). Flow cytometry showed that the proportion of $CD11b^{+}CD163^{+}$ macrophages increased after si-PTEN of macrophages (Figure 6C). Subsequently, secretive level of TGF-β, and MMP9 were detected by ELISA in the culture

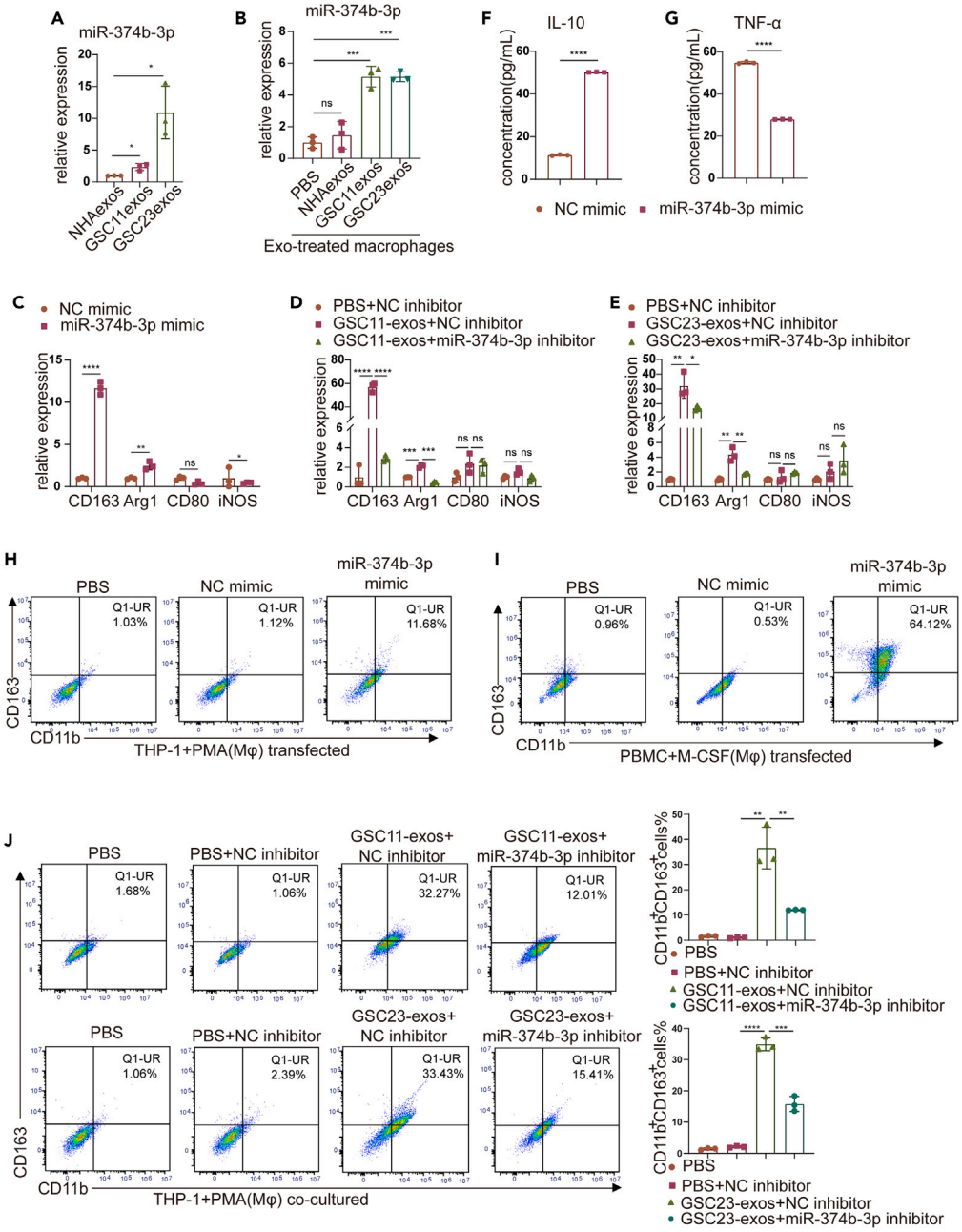

Figure 3. GSCs exosomal miR-374b-3p induced M2 macrophage polarization

(A) MiR-374b-3p levels were analyzed by RT-qPCR in exosomes from NHAs and GSCs (GSC11 and GSC23 cells).

(B) Macrophages were incubated with GSCs-exos or HNAs-exos for 48 h, and miR-374b-3p expression level in macrophages was determined by RT-qPCR.

(C) Macrophages transfected with miR-374b-3p mimics or mimics NC. RT-qPCR was adopted to detect the expression of M2 markers (CD163 and Arg1) and M1 markers (CD80 and iNOS) in macrophages.

(D and E) Macrophages incubated with GSCs-exos and transfected with miR-374b-3p inhibitors or NC inhibitors, RT-qPCR was adopted to detect the expression of M2 markers (CD163 and Arg1) and M1 markers (CD80 and iNOS) in macrophages.

(F and G) The supernatant collected from induced macrophages culture medium was applied to determine IL-10 and TNF-α secretion with ELISA.

(H and I) After transfection with either miR-374b-3p mimics or mimics NC in THP-1 derived macrophages and healthy adult PBMCs-derived macrophages. Flow cytometry were performed to analyze the proportion of CD11b+CD163+ macrophages.

(J) Flow cytometry detection and quantification analysis were performed to compare the proportion of CD11b+CD163+ macrophages in macrophages either incubated with GSCs-exos, or transfected with miR-374b-3p inhibitors, or transfected with NC inhibitors as control, respectively. Data are represented as means ± SD. Statistical analysis of the data from two groups was performed using Student's *t* test. (*p < 0.05; **p < 0.01; ***p < 0.001; ****p < 0.0001, ns: no significance).

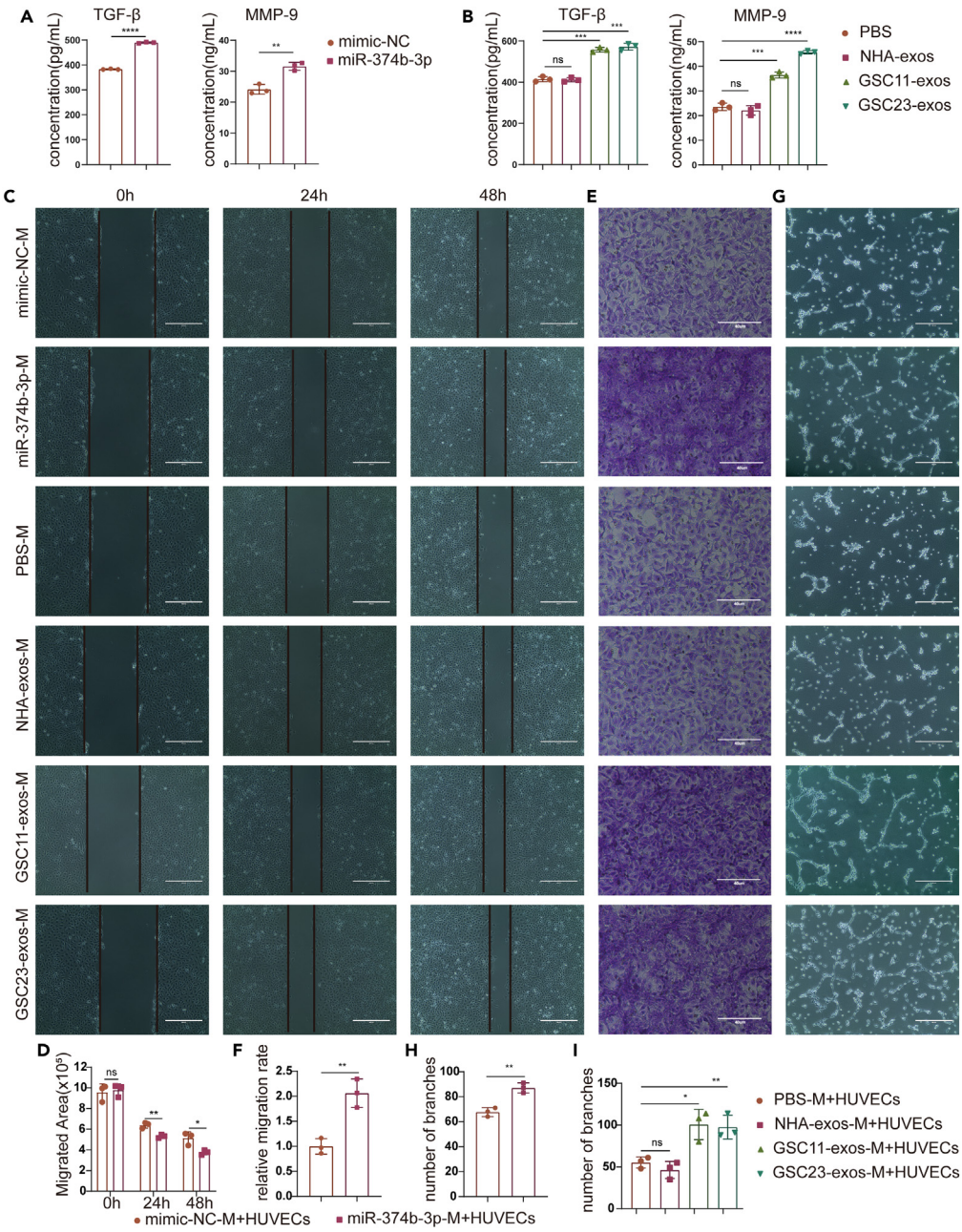

Figure 4. GSCs exosomal miR-374b-3p promoted angiogenesis by inducing M2 polarization of macrophages

(A and B) The supernatant of culture medium from macrophages either transfected with mimics NC, miR-374b-3p mimics, respectively, or incubated with GSCs-exos, HNAs-exos or PBS were examined to determine the secretion of TGF-β and MMP-9 by ELISA.

(C–F) Wound-healing assay and transwell assay were applied to evaluate the lateral migration and the vertical migration capacities of HUVECs, after coculturing with macrophages either transfected with mimics NC, miR-374b-3p mimics, or incubated with GSCs-exos, HNAs-exos, or PBS, respectively. Representative images were shown (Scale bar, 400 μm).

(G–I) Tube formation of HUVECs cocultured with conditioned macrophages was determined (Scale bar, 400 μm). Data are represented as means ± SD. Statistical analysis of the data from two groups was performed using Student's *t* test. (*p < 0.05; **p < 0.01; ***p < 0.001; ****p < 0.0001, ns: no significance).

medium of si-PTEN macrophages. Knockdown of PTEN significantly increased the secretion of some vascular-associated cytokines, such as MMP9 and TGF-β (Figure 6D). To investigate the effect of PTEN knocking down on the angio-promoting role of macrophages, wound-healing assays, transwell assays, and tube formation assays were performed, wound-healing assays and transwell assays indicated that coculture with M2 macrophages transfected si-PTEN significantly increased the migration of endothelial cells HUVECs (Figures 6E, 6F, and S6). Tube

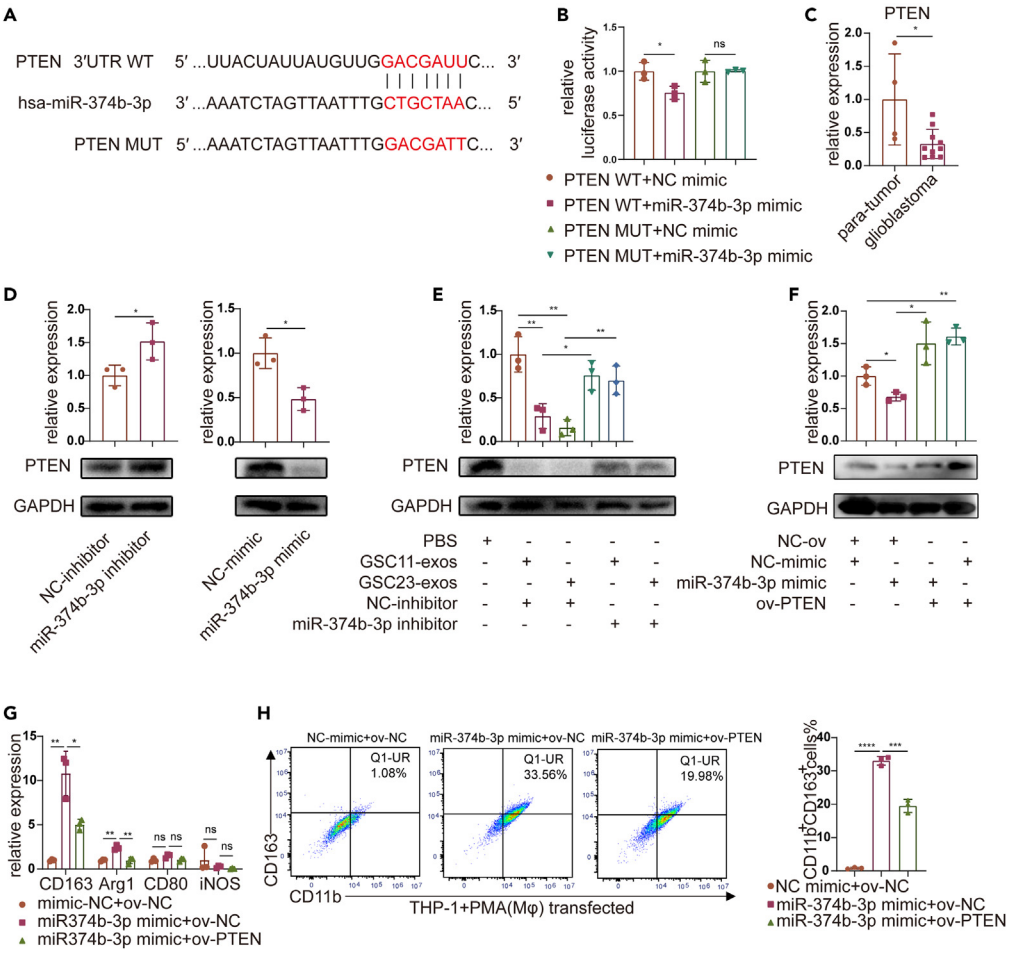

Figure 5. PTEN was the functional target of GSCs exosomal miR-374b-3p in macrophages

(A) Schematic diagram of the wild-type and mutated-type binding site between miR-374b-3p and the PTEN 3′UTR.

(B) Luciferase reporter assay in HEK 293T cells with co-transfection of either wild-type or mutant PTEN 3′UTR, and miR-374b-3p mimics. Luciferase activity was normalized by the ratio of firefly and renilla luciferase signals and determined 48 h after transfection.

(C) The expression levels of PTEN in peri-tumor tissue and glioblastoma tissues were determined by RT-qPCR.

(D) Expression of PTEN in macrophages with miR-374b-3p overexpression or silencing was detected by western blot with quantification analysis.

(E) Expression of PTEN in macrophages either incubated with GSCs-exos, or transfected with miR-374b-3p inhibitors was detected by western blot.

(F) Western blot on expression of PTEN in macrophages either transfected with miR-374b-3p mimics, or transfected with ov-PTEN, respectively.

(G) RT-qPCR was performed to analyze M2 markers (CD163 and Arg1) and M1 markers (CD80 and iNOS) expression in macrophages transfected miR-374b-3p mimics, or ov-PTEN.

(H) The macrophages were transfected with miR-374b-3p mimics, or ov-PTEN, and then $CD11b^{+}CD163^{+}$ macrophages were determined by flow cytometry with quantification analysis. Data are represented as means ± SD. Statistical analysis of the data from two groups was performed using Student's *t* test. (*$p < 0.05$; **$p < 0.01$; ***$p < 0.001$; ****$p < 0.0001$, ns: no significance).

formation assay showed that si-PTEN induced M2 macrophages significantly increased the branches of micro-tubules formed by HUVECs (Figures 6G and 6H). Collectively, these results suggested that GSCs-derived exosomal miR-374b-3p can downregulate PTEN expression, thus polarizing macrophages toward the M2 phenotype, and further enhancing angiogenesis.

To validate the role of GSCs exosomal miR-374b-3p on M2 polarization of macrophages and promoting tumor angiogenesis *in vivo*, macrophages transfected with miR-374b-3p mimics and GSC23 cells were co-implanted into nude mice to establish orthotopic xenografts. Five weeks after inoculation, mice were sacrificed, the entire brains were removed and continuous brain slices were prepared. HE staining showed that macrophages transfected with miR-374b-3p mimics significantly increased intracranial tumors growth, compared with the macrophages transfected with NC mimics (Figure 6I). Furthermore, immunohistochemical staining of Ki67 and CD31 revealed that macrophages transfected with miR-374b-3p mimics resulted in significantly higher proliferative capacity and enhanced angiogenesis in intracerebral xenografts (Figure 6J), and quantified immunohistochemical staining by ImageJ and analyzed statistically (Figure 6K), which showed that miR-374b-3p mimics enhanced the number of Ki67 and CD31 positive cells ratio.

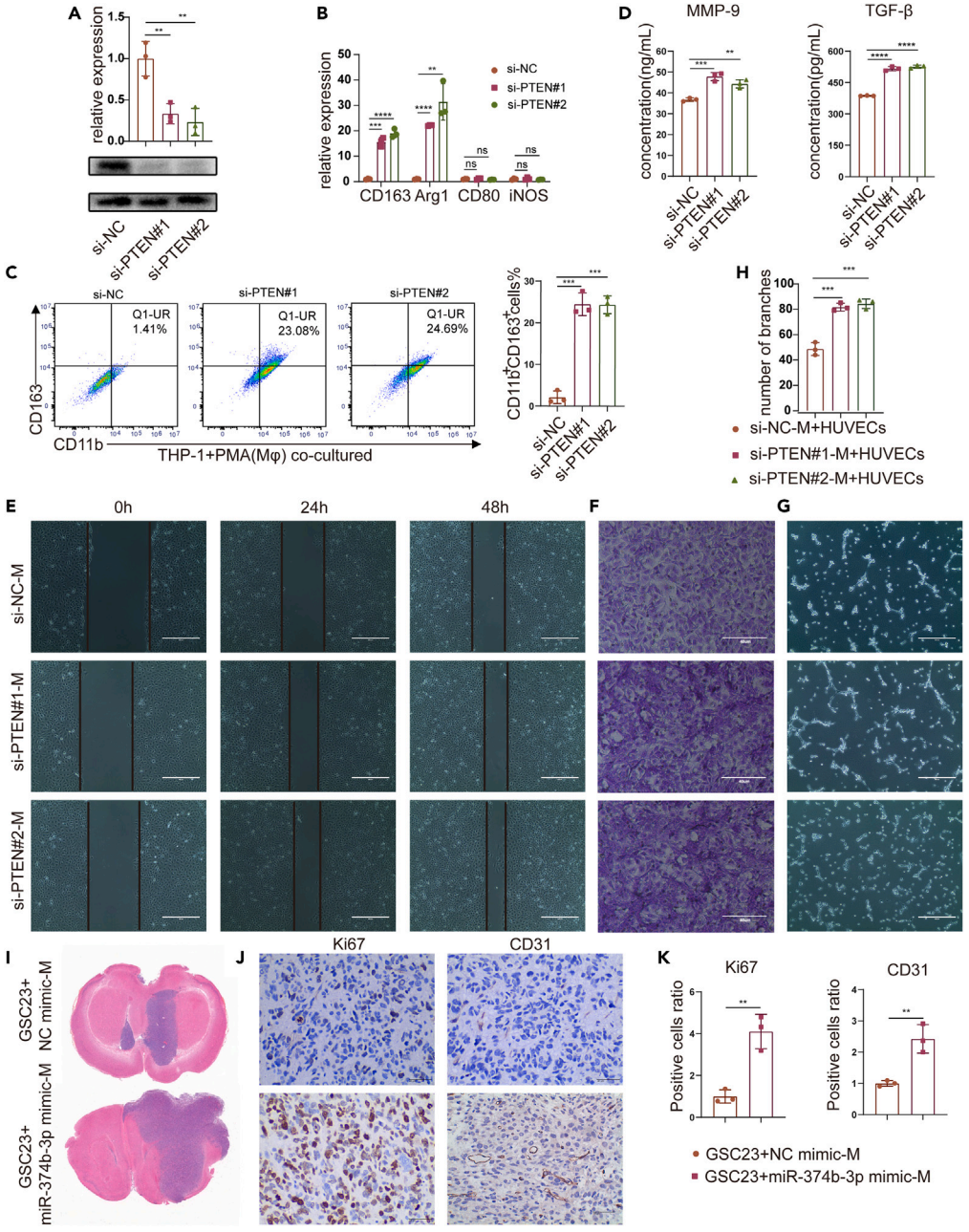

Figure 6. Knockdown of PTEN promoted angiogenesis by inducing M2 polarization of macrophages

(A) Macrophages transfected with si-NC, si-PTEN#1 or si-PTEN#2. RT-qPCR was adopted to detect the expression of M2 markers (CD163 and Arg1) and M1 markers (CD80 and iNOS) in macrophages.

(B) RT-qPCR was performed to analyze expression of M2 markers (CD163 and Arg1) and M1 markers (CD80 and iNOS) in macrophages transfected with si-NC, si-PTEN#1 or si-PTEN#2.

(C) Flow cytometry to analyze the proportion of $CD11b^{+}CD163^{+}$ macrophages transfected with si-NC, si-PTEN#1 or si-PTEN#2.

(D) The supernatants of culture medium from macrophages transfected with si-NC, si-PTEN#1 or si-PTEN#2 were collected to determine the secretion of TGF-β and MMP-9 by ELISA.

(E and F) Wound-healing assay and transwell assay were applied to evaluate the lateral migration and the vertical migration capacities of HUVECs cocultured with macrophages transfected with si-NC, si-PTEN#1 or si-PTEN#2. Representative images were shown (Scale bar, 400 μm).

(G and H) Tube formation of HUVECs cocultured with conditioned macrophages was analyzed (Scale bar, 400 μm).

(I) *In vivo* evaluation of tumorigenesis in orthotopic xenograft nude mice bearing $5X10^{5}$ GSC23 cells with $5X10^{4}$ macrophages transfected with miR-374b-3p mimics. Representative intracranial xenografts of HE staining images were shown (scale bar, 1000 μm).

Figure 6. *Continued*

(J and K) Representative images and quantification of IHC staining for Ki67 and CD31 in sections from the intracranial xenografts (scale bar, 40 μm). Data are represented as means ± SD. Statistical analysis of the data from two groups was performed using Student's *t* test. (**p < 0.01; ***p < 0.001; ****p < 0.0001, ns: no significance).

DISCUSSION

Glioblastoma remains the most common and lethal form of the primary adult cancer in central nervous system,[1] and tumor tissue remodeling is mediated by complicated interactions between tumor stem cells and interstitial cells of TIME.[5] We have observed that some GSCs can enhance tumor vasculatures by transdifferentiation into endothetail-like cells and formation of functional tumor blood vessels *in vivo*.[26] Such kind of vascular mimicry (VM) by GSCs was further investigated.[27,28] The current studies demonstrated that high expression of miR-374b-3p in glioblastoma, GSCs, and GSCs-derived exosomes. Besides, GSCs exosomal miR-374b-3p promoted glioblastoma progression via mediating the crosstalk between GSCs and TAMs, thus promoting tumor angiogenesis. Our findings disclosed a way of GSCs accelerating tumor vessels formation via crosstalk with M2 macrophages (Figure 7).

Exosomes are extracellular vesicles rich in functional molecules such as proteins, lipids, and nucleic acids.[15,29] In recent years, tumor cells-derived exosomal miRNA have been found to play critical roles in regulating cell proliferation, metastasis, angiogenesis, drug resistance, and immune escape.[29,30] MiR-374b-3p has been reported to be aberrantly expressed in human melanoma[31] and play an important promoting role in both tumor growth and angiogenesis of clear cell renal cell carcinoma (ccRCC).[32] They reported that circAFAP1 was a miRNA sponge for miR-374b-3p targeting VEGFA to promote ccRCC growth and angiogenesis. The vascular promotion ability of miR-374b-3p was validated by adding the supernatant of the relative ccRCC cells to HUVEC cells, and tumor cell derived miR-374b-3p can be engulfed by endothelial cells, then upregulated VEGFA expression, leading to initiation of vascularization. Our results disclosed the vascular promotion ability of miR-374b-3p by indirect cocultured of GSC exosomal miR-374b-3p induced M2 macrophages with endothelial cells. Our data also disclosed that peripheral blood serum and tumor tissue samples of glioblastoma patients exhibited apparently higher levels of miR-374b-3p, which enriched in GSCs exosomes as well.

Owing to the wide landscape of genomic alterations and limited therapeutic success in targeting tumor cells, recent studies have focused on deep understanding and possibly targeting the microenvironment to repress tumors development.[33] TAMs are among the most common tumor stromal cells in TIME and play significant roles in modulating growth and invasiveness of glioblastoma.[7] Previous studies have disclosed that TAMs can be functionally categorized into at least tumour-supportive (M2 type) macrophages and tumor suppressive (M1 type) macrophages.[10–12] While M1 type display an immune surveillance function, M2 type are generally immune-suppressive and facilitate malignant behaviors of glioblastoma.[21,25] However, due to the heterogeneity of macrophages in glioblastoma micro-environment, macrophages should not be simply classified into only the two types of activated macrophages termed M1 and M2.[34] But the current advances of macrophages heterogeneity were not enough to support new precise classification criteria for macrophages.

Since there is currently no recognized method for precise functional classification of macrophages that does not rely on the M1/2 system in cancer research fields, and the descriptions relevant to tumor promoting function of glioma-associated macrophages mainly have to depend on the current functional characteristics of M2 macrophages.[12,25] Therefore, both pro-inflammation (M1) and pro-tumor (M2) macrophages existed in tumor microenvironment based on the simple M1/M2 typing system with obvious limitation, and "M2-like" macrophages are still used as an alternative model of TAMs in most studies of various tumors, including glioma. New classification criteria based on precise depicting the heterogeneity of TAMs will greatly promote the relevant studies.

Tumor cells-derived exosomes carry variety of molecules modulating metastasis, angiogenesis, and drug resistance to enhance tissue remodeling of tumor.[34] Previous studies have proved that exosomal miRNAs promoted angiogenesis and tumor progression by regulating the interactions between tumor cells and TAMs.[35,36] Exosomal miR-519a-3p derived from gastric cancer promoted tumor angiogenesis by inducing M2 polarization of macrophages,[36] and exosomal miR-301a-3p secreted from esophageal squamous carcinoma cells induced M2 macrophage polarization and promoted angiogenesis via secretion of angiogenic factors VEGFA and MMP9.[37] The current studies disclosed that intracellular high level of miR-374b-3p in GSCs can be delivered to macrophages via GSCs-exos, resulting in M2 polarization and PTEN downregulation of macrophages, which further promoted migration and tubule formation abilities of endothelial cells by secreting pro-angiogenic cytokines TGF-β and MMP-9.

PTEN is an important tumor suppressor with both lipid phosphatase and protein phosphatase activities, which regulates multiple cell functions, including cell proliferation, differentiation, and angiogenesis.[38,39] PTEN deletion results in enhanced recruitment of macrophages into tumor microenvironment and promote macrophage M2 polarization.[40,41] Aberrant downregulation of PTEN is closely associated with tumorigenesis. Furthermore, PTEN can serve as a functional target of GSCs exosomal miR-374b-3p in macrophages, and knockdown of PTEN in macrophages induced M2 polarization and promoted angiogenesis of glioblastoma by secrete TGF-β and MMP-9, disclosed by our investigations, which highlighted that glioblastoma development is a complex process involving sophisticated crosstalk between GSCs and macrophages during tissue remodeling of glioblastoma.

Limitations of the study

While we showed that M2 macrophages polarized by GSC exosomal miR-374b-3p and si-PTEN secrete more MMP9 and TGF-β, how they secreted and then promoted angiogenesis remains unclear. One common issue associated with immune-deficiency mouse models in glioblastoma research fields is the lack of T lymphocytes, which limits the interpretation of immune-related experimental data.

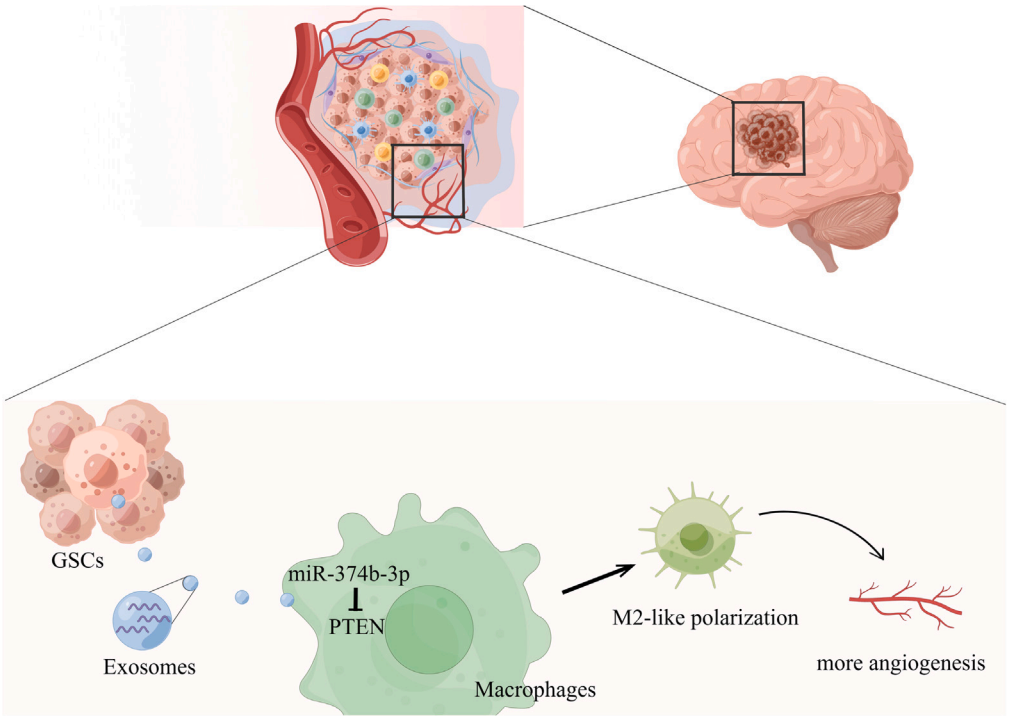

Figure 7. Molecular mechanism diagram by figdraw

Glioblastoma stem cells (GSCs) exosomal miR-374b-3p induces M2 polarization of macrophage into TAMs via targeting PTEN, and further facilitates angiogenic ability of HUVECs to contribute glioblastoma vasculature.

STAR★METHODS

Detailed methods are provided in the online version of this paper and include the following:

- KEY RESOURCES TABLE
- RESOURCE AVAILABILITY
  - Lead contact
  - Materials availability
  - Data and code availability
- EXPERIMENTAL MODEL AND STUDY PARTICIPANT DETAILS
  - Patients and specimens
  - Animal studies
  - Ethics approval and consent to participate
  - Consent for publication
  - Cultured cells
  - Intracranial tumor model
- METHOD DETAILS
  - Isolation and purification of exosomes
  - Electron microscopy and nanoparticle tracking analysis
  - Engulf of exosomes by macrophages
  - Cell transfection
  - RT-qPCR
  - Western blot
  - Wound healing assay
  - Transwell assay
  - Tube formation assay
  - ELISA
  - Flow cytometry
  - Dual-luciferase reporter assay

- Immuno-histochemical staining (IHC) and hematoxylin-eosin (HE) staining
- QUANTIFICATION AND STATISTICAL ANALYSIS

SUPPLEMENTAL INFORMATION

Supplemental information can be found online at https://doi.org/10.1016/j.isci.2024.109270.

ACKNOWLEDGMENTS

The authors would like to thank Dr. Rongrong Cao for helping to execute details of the experiment that required assistance. This work was supported by grants from the Jiangsu Province Key Research and Development Program: Social Development Project (grant/award number: BE2021653), Key Project of Jiangsu Health Commission (grant/award number: ZDB2020016) and National Natural Science Foundation of China (82203637).

AUTHOR CONTRIBUTIONS

J.D.: conceived the study and participated in the study design. S.H., Z.X., P.Z., N.Y., and A.W.: performed cell culture, tubule formation, HUVEC migration, flow cytometry, RT-qPCR, ELISA, western blot, and luciferase assay. S.H., Z.Z., T.Z., X.Z., and Z.L.: performed bioinformatics analysis, constructed animal models, HE and IHC staining. Primer design and plasmid construction were carried out by L.L., X.L., and Y.S. P.Z., Z.X., X.Z., and Z.L. analyzed the data, sorted the charts, and wrote the manuscript. The final draft was read and approved by all authors.

DECLARATION OF INTERESTS

The authors declared no competing interests.

Received: October 7, 2023
Revised: January 30, 2024
Accepted: February 14, 2024
Published: February 22, 2024

REFERENCES

1. Ostrom, Q.T., Price, M., Neff, C., Cioffi, G., Waite, K.A., Kruchko, C., and Barnholtz-Sloan, J.S. (2022). CBTRUS Statistical Report: Primary Brain and Other Central Nervous System Tumors Diagnosed in the United States in 2015-2019. Neuro Oncol. *24*.
2. Krex, D., Klink, B., Hartmann, C., von Deimling, A., Pietsch, T., Simon, M., Sabel, M., Steinbach, J.P., Heese, O., Reifenberger, G., et al. (2007). Long-term survival with glioblastoma multiforme. Brain *130*, 2596–2606.
3. Man, J., Shoemake, J.D., Ma, T., Rizzo, A.E., Godley, A.R., Wu, Q., Mohammadi, A.M., Bao, S., Rich, J.N., and Yu, J.S. (2015). Hyperthermia Sensitizes Glioma Stem-like Cells to Radiation by Inhibiting AKT Signaling. Cancer Res. *75*, 1760–1769.
4. Chen, J., Li, Y., Yu, T.S., McKay, R.M., Burns, D.K., Kernie, S.G., and Parada, L.F. (2012). A restricted cell population propagates glioblastoma growth after chemotherapy. Nature *488*, 522–526.
5. He, Z., Ruan, X., Liu, X., Zheng, J., Liu, Y., Liu, L., Ma, J., Shao, L., Wang, D., Shen, S., et al. (2019). FUS/circ_002136/miR-138-5p/SOX13 feedback loop regulates angiogenesis in Glioma. J. Exp. Clin. Cancer Res. *38*, 65.
6. Kumar, S., Bar-Lev, L., Sharife, H., Grunewald, M., Mogilevsky, M., Licht, T., Goveia, J., Taverna, F., Paldor, I., Carmeliet, P., and Keshet, E. (2022). Identification of vascular cues contributing to cancer cell stemness and function. Angiogenesis *25*, 355–371.
7. Cheng, N., Bai, X., Shu, Y., Ahmad, O., and Shen, P. (2021). Targeting tumor-associated macrophages as an antitumor strategy. Biochem. Pharmacol. *183*, 114354.
8. Thorsson, V., Gibbs, D.L., Brown, S.D., Wolf, D., Bortone, D.S., Ou Yang, T.-H., Porta-Pardo, E., Gao, G.F., Plaisier, C.L., Eddy, J.A., et al. (2018). The Immune Landscape of Cancer. Immunity *48*, 812–830.e14.
9. Iv, M., Samghabadi, P., Holdsworth, S., Gentles, A., Rezaii, P., Harsh, G., Li, G., Thomas, R., Moseley, M., Daldrup-Link, H.E., et al. (2019). Quantification of Macrophages in High-Grade Gliomas by Using Ferumoxytol-enhanced MRI: A Pilot Study. Radiology *290*, 198–206.
10. Cassetta, L., and Pollard, J.W. (2018). Targeting macrophages: therapeutic approaches in cancer. Nat. Rev. Drug Discov. *17*, 887–904.
11. Ostuni, R., Kratochvill, F., Murray, P.J., and Natoli, G. (2015). Macrophages and cancer: from mechanisms to therapeutic implications. Trends Immunol. *36*, 229–239.
12. Shi, Y., Ping, Y.-F., Zhou, W., He, Z.-C., Chen, C., Bian, B.-S.-J., Zhang, L., Chen, L., Lan, X., Zhang, X.-C., et al. (2017). Tumour-associated macrophages secrete pleiotrophin to promote PTPRZ1 signalling in glioblastoma stem cells for tumour growth. Nat. Commun. *8*, 15080.
13. Zhou, W., Ke, S.Q., Huang, Z., Flavahan, W., Fang, X., Paul, J., Wu, L., Sloan, A.E., McLendon, R.E., Li, X., et al. (2015). Periostin secreted by glioblastoma stem cells recruits M2 tumour-associated macrophages and promotes malignant growth. Nat. Cell Biol. *17*, 170–182.
14. Lewis, C.E., and Pollard, J.W. (2006). Distinct role of macrophages in different tumor microenvironments. Cancer Res. *66*, 605–612.
15. Xu, R., Rai, A., Chen, M., Suwakulsiri, W., Greening, D.W., and Simpson, R.J. (2018). Extracellular vesicles in cancer - implications for future improvements in cancer care. Nat. Rev. Clin. Oncol. *15*, 617–638.
16. Zhang, Z.G., Buller, B., and Chopp, M. (2019). Exosomes - beyond stem cells for restorative therapy in stroke and neurological injury. Nat. Rev. Neurol. *15*, 193–203.
17. Jeppesen, D.K., Fenix, A.M., Franklin, J.L., Higginbotham, J.N., Zhang, Q., Zimmerman, L.J., Liebler, D.C., Ping, J., Liu, Q., Evans, R., et al. (2019). Reassessment of Exosome Composition. Cell *177*, 428–445.e18.
18. Tkach, M., and Théry, C. (2016). Communication by Extracellular Vesicles: Where We Are and Where We Need to Go. Cell *164*, 1226–1232.
19. Tan, S., Xia, L., Yi, P., Han, Y., Tang, L., Pan, Q., Tian, Y., Rao, S., Oyang, L., Liang, J., et al. (2020). Exosomal miRNAs in tumor microenvironment. J. Exp. Clin. Cancer Res. *39*, 67.
20. Huang, S., Liu, L., Xu, Z., Liu, X., Wu, A., Zhang, X., Li, Z., Li, S., Li, Y., Yuan, J., et al. (2023). Exosomal miR-6733-5p mediates cross-talk between glioblastoma stem cells and macrophages and promotes glioblastoma multiform progression synergistically. CNS Neurosci. Ther. *29*, 3756–3773.
21. Sica, A., Larghi, P., Mancino, A., Rubino, L., Porta, C., Totaro, M.G., Rimoldi, M., Biswas, S.K., Allavena, P., and Mantovani, A. (2008). Macrophage polarization in tumour progression. Semin. Cancer Biol. *18*, 349–355.
22. Riabov, V., Gudima, A., Wang, N., Mickley, A., Orekhov, A., and Kzhyshkowska, J. (2014).

Role of tumor associated macrophages in tumor angiogenesis and lymphangiogenesis. Front. Physiol. *5*, 75.
23. Vempati, P., Popel, A.S., and Mac Gabhann, F. (2014). Extracellular regulation of VEGF: isoforms, proteolysis, and vascular patterning. Cytokine Growth Factor Rev. *25*, 1–19.
24. Pardali, E., Goumans, M.J., and ten Dijke, P. (2010). Signaling by members of the TGF-beta family in vascular morphogenesis and disease. Trends Cell Biol. *20*, 556–567.
25. Zhao, S., Mi, Y., Guan, B., Zheng, B., Wei, P., Gu, Y., Zhang, Z., Cai, S., Xu, Y., Li, X., et al. (2020). Tumor-derived exosomal miR-934 induces macrophage M2 polarization to promote liver metastasis of colorectal cancer. J. Hematol. Oncol. *13*, 156.
26. Dong, J., Zhao, Y., Huang, Q., Fei, X., Diao, Y., Shen, Y., Xiao, H., Zhang, T., Lan, Q., and Gu, X. (2011). Glioma stem/progenitor cells contribute to neovascularization via transdifferentiation. Stem Cell Rev. Rep. *7*, 141–152.
27. Wang, R., Chadalavada, K., Wilshire, J., Kowalik, U., Hovinga, K.E., Geber, A., Fligelman, B., Leversha, M., Brennan, C., and Tabar, V. (2010). Glioblastoma stem-like cells give rise to tumour endothelium. Nature *468*, 829–833.
28. Ricci-Vitiani, L., Pallini, R., Biffoni, M., Todaro, M., Invernici, G., Cenci, T., Maira, G., Parati, E.A., Stassi, G., Larocca, L.M., and De Maria, R. (2010). Tumour vascularization via endothelial differentiation of glioblastoma stem-like cells. Nature *468*, 824–828.
29. Zhang, X., Yuan, X., Shi, H., Wu, L., Qian, H., and Xu, W. (2015). Exosomes in cancer: small particle, big player. J. Hematol. Oncol. *8*, 83.
30. Taylor, D.D., and Gercel-Taylor, C. (2011). Exosomes/microvesicles: mediators of cancer-associated immunosuppressive microenvironments. Semin. Immunopathol. *33*, 441–454.
31. Ou, Y., Dai, X., Chen, X., Chen, Y., Wu, S., Zhou, Q., Yang, C., and Jiang, H. (2022). Circ-AFAP1 promote clear cell renal cell carcinoma growth and angiogenesis by the Circ-AFAP1/miR-374b-3p/VEGFA signaling axis. Cell Death Dis. *8*, 68.
32. Hanniford, D., Zhong, J., Koetz, L., Gaziel-Sovran, A., Lackaye, D.J., Shang, S., Pavlick, A., Shapiro, R., Berman, R., Darvishian, F., et al. (2015). A miRNA-Based Signature Detected in Primary Melanoma Tissue Predicts Development of Brain Metastasis. Clin. Cancer Res. *21*, 4903–4912.
33. Bach, D.-H., Hong, J.-Y., Park, H.J., and Lee, S.K. (2017). The role of exosomes and miRNAs in drug-resistance of cancer cells. Int. J. Cancer *141*, 220–230.
34. Murray, P.J., Allen, J.E., Biswas, S.K., Fisher, E.A., Gilroy, D.W., Goerdt, S., Gordon, S., Hamilton, J.A., Ivashkiv, L.B., Lawrence, T., et al. (2014). Macrophage activation and polarization: nomenclature and experimental guidelines. Immunity *41*, 14–20.
35. Qiu, S., Xie, L., Lu, C., Gu, C., Xia, Y., Lv, J., Xuan, Z., Fang, L., Yang, J., Zhang, L., et al. (2022). Gastric cancer-derived exosomal miR-519a-3p promotes liver metastasis by inducing intrahepatic M2-like macrophage-mediated angiogenesis. J. Exp. Clin. Cancer Res. *41*, 296.
36. Shou, Y., Wang, X., Chen, C., Liang, Y., Yang, C., Xiao, Q., Li, H., Wang, S., Shu, J., Tian, X., and Chen, K. (2022). Exosomal miR-301a-3p from esophageal squamous cell carcinoma cells promotes angiogenesis by inducing M2 polarization of macrophages via the PTEN/PI3K/AKT signaling pathway. Cancer Cell Int. *22*, 153.
37. Affo, S., Yu, L.-X., and Schwabe, R.F. (2017). The Role of Cancer-Associated Fibroblasts and Fibrosis in Liver Cancer. Annu. Rev. Pathol. *12*, 153–186.
38. Garcia-Cao, I., Song, M.S., Hobbs, R.M., Laurent, G., Giorgi, C., de Boer, V.C.J., Anastasiou, D., Ito, K., Sasaki, A.T., Rameh, L., et al. (2012). Systemic elevation of PTEN induces a tumor-suppressive metabolic state. Cell *149*, 49–62.
39. Song, M.S., Salmena, L., and Pandolfi, P.P. (2012). The functions and regulation of the PTEN tumour suppressor. Nat. Rev. Mol. Cell Biol. *13*, 283–296.
40. Chen, P., Zhao, D., Li, J., Liang, X., Li, J., Chang, A., Henry, V.K., Lan, Z., Spring, D.J., Rao, G., et al. (2019). Symbiotic Macrophage-Glioma Cell Interactions Reveal Synthetic Lethality in PTEN-Null Glioma. Cancer Cell *35*, 868–884.e6.
41. Ni, X., Wu, W., Sun, X., Ma, J., Yu, Z., He, X., Cheng, J., Xu, P., Liu, H., Shang, T., et al. (2022). Interrogating glioma-M2 macrophage interactions identifies Gal-9/Tim-3 as a viable target against PTEN-null glioblastoma. Sci. Adv. *8*, eabl5165.

STAR★METHODS

KEY RESOURCES TABLE

REAGENT or RESOURCE	SOURCE	IDENTIFIER
Antibodies		
Rabbit monoclonal anti-GAPDH	proteintech	Cat# 60004-1-Ig; RRID: AB_2107436
Rabbit monoclonal anti-CD9	abcam	Cat# ab263019; RRID: N/A
Rabbit monoclonal anti-HSP70	abcam	Cat# ab181606; RRID: AB_2910093
Rabbit monoclonal anti-Calnexin	abcam	Cat# ab133615; RRID: AB_2864299
Rabbit monoclonal anti-PTEN	abcam	Cat# ab267787; RRID: AB_2923364
monoclonal anti-CD163-PE	Biolegend	Cat# 333606 (also 333605); RRID: AB_1134002
monoclonal anti-CD11b-FITC	Biolegend	Cat# 301330 (also 301329); RRID: AB_2561703
Anti -Ki67 Rabbit mAb	Servicebio	Cat# GB13030-2; RRID: AB_2943459
anti- CD31	abcam	Cat# ab182981; RRID: AB_2920881
anti- F4/80	proteintech	Cat# 28463-1-AP; RRID: AB_2881149
Chemicals, peptides, and recombinant proteins		
Phorbol-12-myristate-13-acetate(PMA)	Sigma-Aldrich	Lot#SLBX8889
macrophage colony stimulating factor (M-CSF)	PeproTech	Lot#300-25
Critical commercial assays		
IL-10 and TNF-α ELISA kit	Biolengend	430607 and 430207
TGF-β and MMP-9 ELISA kit	Jiangsu meibiao biology	MB-3393A and MB-3558A
NovoStart SYBR qPCR SuperMix Plus Kit	Novoprotein	2610
RevertAid First Strand cDNA Synthesis Kit	ThermoFisher	K1622
Dual-Luciferase Reporter Assay	Promega	E1910
Deposited data		
Raw and analyzed data	This paper	GEO:GSE139031 and GSE113740
Experimental models: Cell lines		
Human: GSC11 and GSC23 cells	M.D. Anderson Cancer Center	N/A
Human astrocytes NHAs	ATCC	N/A
THP-1 cell line	ATCC	N/A
Experimental models: Organisms/strains		
Mouse: female BALB/c nude mice	SLAC ANIMAL	N/A
Oligonucleotides		
siRNA targeting sequence: si- PTEN #1: sense 5′-GGUGUAAUGAUAUGUGCAUTT -3′ antisense 5′- AUGCACAUAUCAUUACACCTT -3′	This paper	N/A
siRNA targeting sequence: si- PTEN #2: sense 5′- GCUACCUGUUAAAGAAUCATT-3′ antisense 5′- UGAUUCUUUAACAGGUAGCTT -3′	This paper	N/A
miR-374b-3p mimics: sense 5′- CUUAGCAGGUUGUAUUAUCAUU-3′ antisense 5′- UGAUAAUACAACCUGCUAAGUU-3′	This paper	N/A
miR-374b-3p inhibitor: sense 5′-AAUGAUAAUACAACCUGCUAAG-3′	This paper	N/A

(*Continued on next page*)

Continued

REAGENT or RESOURCE	SOURCE	IDENTIFIER
Recombinant DNA		
Plasmid: PTEN	This paper	N/A
Software and algorithms		
ImageJ	Image Processing and Analysis in Java	https://imagej.nih.gov/ij/
GraphPad Prism 8	GraphPad	https://www.graphpad.com/
FlowJo software 10.8.1	Tree Star	https://www.flowjo.com/

RESOURCE AVAILABILITY

Lead contact

Further information and requests for resources and reagents should be directed to and will be fulfilled by the lead contact, Jun Dong (dongjun@suda.edu.cn).

Materials availability

All unique/stable reagents generated in this study are available from the lead contact with a completed Materials Transfer Agreement.

Data and code availability

- This paper does not report any original code.
- The data reported in this paper will be shared by the lead contact upon reasonable request.
- Any additional information required to reanalyze the data reported in this paper is available from the lead contact upon reasonable request.

EXPERIMENTAL MODEL AND STUDY PARTICIPANT DETAILS

Patients and specimens

The patient samples used in this study were collected at the Second Affiliated Hospital of Soochow University. We included a total of 11 patients with GBM (Grade IV), aged 49–77 years, with no restriction on gender, ancestry, race or ethnicity or socioeconomic information. A small amount of para-tumoral tissues was obtained from establishing the surgical pathway to expose the intracerebral tumor with informed consent and ethical approval of the Second Affiliated Hospital of Soochow University. The pathological diagnosis of glioblastoma was independently achieved by two senior and experienced pathologists according to World Health Organization (WHO) pathological criteria at the Department of Neurosurgery, the Second Affiliated Hospital of Soochow University. The samples were de-identified before being processed.

Animal studies

Four-week-old female BALB/c nude mice provided by SLAC ANIMAL (Shanghai, China) were housed in a specific pathogen-free (SPF) animal room with a 12-h light/12-h dark cycle and free access to food and water. All animal experiment protocols were approved by the Institutional Animal Care and Use Committee of Soochow University (Suzhou, China).

Ethics approval and consent to participate

This study was approved by the Ethics Committee of the Second Affiliated Hospital of Soochow University (2022148). All patients provided written informed consent.

Consent for publication

Written informed consent for publication was obtained from all the participants.

Cultured cells

Human peripheral blood mononu-clear cells (PBMCs) were isolated via density gradient centrifugation using Ficoll-Paque (TBDScience LTS1077) at 2000 g for 25 min using minimum acceleration and no brake. PBMC fractions were washed in sterile PBS after lysing erythrocytes (CWBIO, CW0613) and plated to select for adherent cells. Non-adherent cells were washed away after 6 h and the remaining cells incubated in RPMI 1640 medium (Gibco) supplemented with 10% heat-inactivated pooled human serum (Sigma) and 40 ng/mL macrophage colony-stimulating factor (M-CSF, PeproTech, 300-25). Medium changed every 3 days until the cells differentiated into macrophages by 7 days. Human glioma stem cell lines GSC11 and GSC23 (M.D. Anderson Cancer Center) were cultured in Dulbecco's modified Eagle's medium (DMEM)/F12

medium (Gibco, USA) containing 20 ng/mL basic fibroblast growth factor (bFGF) (Gibco) and 20 ng/mL epidermal growth factor (EGF) (Gibco). Human astrocytes NHAs (ATCC) were cultured in Dulbecco's modified Eagle medium (DMEM) (Gibco) supplemented with 10% heat-inactivated fetal bovine serum (FBS, Invitrogen). THP-1 cell line (ATCC) was cultured in RPMI 1640 medium (Gibco) supplemented with 10% heat-inactivated fetal bovine serum (FBS, Invitrogen), then incubated with 100 ng/mL phorbol-12-myristate-13-acetate (PMA; Sigma-Aldrich, USA) for 24-48 h to induce differentiation into macrophages.All cells were maintained in a humidified chamber containing 5% CO_2 at 37°C.

Intracranial tumor model

For evaluation the pro-tumor effect of GSCs-exos *in vivo*, female BALB/c nude mice (4 weeks old, 15–20 g) were applied, and randomly assigned into two groups. There were three mice per group. 5x105 SNB19 cells were injected into the right caudate nucleus of nude mice. mice were intravenously injected with 50 μL PBS or equal volumes of GSC23-exos (20 μg) through tail vein injection every three days for 2 weeks.For evaluation of the role of miR-374b-3p *in vivo*, 5x105 GSC23 cells were mixed with 5x104 conditioned macrophages transfected with miR-374b-3p mimics, then inoculated into the right caudate nucleus of nude mice. Mice were euthanized when obvious neurological symptoms appeared. Then the whole brains of tumor-bearing mice were harvested, paraformaldehyde-fixed, paraffin-embedded, and sectioned coronally from anterior to posterior of brain.

METHOD DETAILS

Isolation and purification of exosomes

The culture supernatant was collected from GSCs (GSC11 or GSC23 cells) culture in DMEM/F12 medium containing 20 ng/mL bFGF and EGF for 4 days. NHA-exos were harvested from culture medium of NHAs (DMEM supplemented with 10% exosome-depleted FBS) for 2 days under 5% CO_2 at 37°C. Briefly, the collected culture medium was centrifuged at 2000 g for 30 min, then 12,000 g for 45 min to remove cell debris and large vesicles. For exosome purification, the supernatant was ultracentrifuged at 100,000 g for 70 min at 4°C to collect the pellet, then was resuspended in 50–100 μL PBS for the subsequent studies. The concentration of exosomes was detected using a BCA Protein Assay (Beyotime). For exosome addition, the culture medium of recipient cells was supplemented with purified exosomes at 20 μg/mL unless otherwise specified.

Electron microscopy and nanoparticle tracking analysis

Exosomes to be examined by TEM were applied to assess the morphology of exosomes. In brief, exosomes (10 μg) fixed with 4% formaldehyde were placed on copper grids, washed with filtered PBS, and stained with uranyl acetate solution. After 24 h of incubation, samples were analyzed with TEM (Hitachi HT-7700). Besides, the size distribution and concentration were detected by NTA (ZetaView PMX 110, Particle Metrix).

Engulf of exosomes by macrophages

Purified exosomes were collected and labeled with PKH26 Red Fluorescent membrane linker dye (Sigma-Aldrich) according to the manufacturer's instructions. THP-1 cells were seeded in eight-well chamber slides (5000 cells/well) and pretreated with PMA for 24 h. Then, 10 μg exosomes were incubated with PKH26 dye at room temperature for 5 min. After centrifuged at 10,000 g for 30 min at 4°C, the labeled exosome pellets were resuspended and added to THP-1 derived macrophages for exosomes uptake studies. After incubation for 8 h at 37°C, cells were fixed, stained with DAPI (Invitrogen), and examined under confocal microscope (Zeiss).

Cell transfection

The miR-374b-3p mimics/inhibitors and the si-PTEN (GenePharma, Shanghai, China) were transiently transfected using siRNA-mate (GenePharma, Shanghai, China) according to the manufacturer's instructions. Sequence information was available in key resources table. Plasmid vector overexpressed PTEN (FuBio, Suzhou, China) was transfected with Lipofectamine 3000 (Invitrogen, Carlsbad, CA) following the manufacturer's instructions.

RT-qPCR

Total RNA was extracted from cells or tissues with TRIzol (Yesen, China), then was transcribed into cDNA using NovoScript Plus All-in-one 1st Strand cDNA Synthesis SuperMix (gDNA Purge) (Novoprotein, Shanghai, China) according to the manufacturer's protocols. The miRNAs were reversed transcribed via miRNA-specific stem-loop RT primers with RevertAid First Strand cDNA Synthesis Kit (ThermoFisher, USA), and cDNA was amplified using NovoStart SYBR qPCR SuperMix Plus Kit (Novoprotein, Shanghai, China). RT-qPCR was performed according to the manufacturer's protocol. The relative expression of miRNA and mRNA was normalized to U6 and GAPDH, respectively. Primer information is shown in key resources table. The final data were analyzed using the $2^{-\Delta\Delta Ct}$ method. The qPCR assay was performed with three technical replicates, and at least three independent biological replicates were performed.

Western blot

Cells or exosomes were lysed in radioimmune precipitation assay (RIPA) lysis buffer (Beyotime) containing protease inhibitor cocktails (Abcam). Protein concentration was determined with BCA Protein Assay Kit (Beyotime, China). A total of 20–30 μg of protein sample was subjected to SDS-PAGE gel, then transferred onto 0.22-mm polyvinylidene difluoride (PVDF) membranes (Millipore). The membrane was blocked in 5% non-fat milk for 2 h at room temperature and incubated with the corresponding primary antibodies at 4°C overnight, following by incubation with the horseradish peroxidase-conjugated (HRP) secondary antibody for 2 h at room temperature. Finally, the membrane was detected using FDbio-Femto ECL (Fudebio, Hangzhou, China) and a chemiluminescence system (Bio-Rad, USA). The primary antibodies for Western blot were anti-GAPDH (1:10,000; proteintech, 60004-1-Ig), anti-CD9 (1:1000; abcam, ab263019), anti-PTEN (1:1000; abcam, ab267787), anti-HSP70 (1:1000; abcam, ab181606) and anti-Calnexin (1:1000; abcam, ab133615), respectively.

Wound healing assay

In vitro coculture system was applied. $1X10^5$ Human umbilical vein endothelial cells (HUVECs) were seeded in the upper chamber (diameter = 0.4 μm; Corning, USA), $2X10^5$ macrophages, either incubated with 20 μg/mL GSCs-exos or transfected with miR-374b-3p mimics, si-PTEN were added to the lower chamber. After 48 h of coculture, HUVECs were harvested from the upper chamber, then seeded in a six-well plate, culture in medium for 24 h. A 10 μL pipette tip was applied to make wounds in the cell monolayer. Then, cells were washed with PBS and cultured in medium without FBS. Twenty-four and 48 h later, cells were observed under an inverted microscope (AMG, USA). Images of the wounded area were captured and analyzed via ImageJ.

Transwell assay

Transwell inserts (8.0 μm, Corning) were used to evaluate the migration ability of HUVECs. The upper chambers contained 300 μL of 2% FBS-containing medium, while the lower chambers contained 600 μL of 10% FBS-containing medium. After 48 h, cells in the upper chamber were wiped, cells that migrated into the lower chamber were captured under microscope (AMG EVOS, USA).

Tube formation assay

Matrigel (Corning, USA) was first thawed at 4°C and spread into 24-well plates (200 μL per well) at 37°C for 30 min to form gel. Then HUVECs (1×10^5/well) were seeded. After 6 h incubation, tube formation was photographed under microscope (AMG, USA), and the number of branches extending from the tubes was counted and analyzed with ImageJ.

ELISA

Cell culture medium of macrophages was collected 48 h after the indicated interventions. Secretion of IL-10 and TNF-α was determined with ELISA (Biolengend, 430607, 430207), as well as TGF-β and MMP-9(Jiangsu meibiao biology, MB-3393A, MB-3558A), according to the manufacturer's instructions.

Flow cytometry

To detect $CD11b^+CD163^+$macrophages, anti-CD11b-FITC (Biolegend, 301330) and anti-CD163-PE (Biolegend, 333606) monoclonal antibodies were applied to sort cells with Cytoflex flow cytometer (Beckman Coulter, Krefeld, Germany). Cells were gated based on FSC and SSC characteristics. All data was analyzed with FlowJo software (FlowJo 10.8.1; FlowJo, Ashland, OR, USA).

Dual-luciferase reporter assay

The 293T cells were cotransfected with wild-type or mutant PTEN 3′UTR pGL3 plasmid (FuBio, Suzhou, China) and miR-374b-3p mimics or control using Lipofectamine 3000 (Invitrogen). Luciferase activity was detected with the Dual-Luciferase Reporter Assay System (Promega) following the manufacturer's instructions.

Immuno-histochemical staining (IHC) and hematoxylin-eosin (HE) staining

The whole brain of tumor-bearing mice was fixed with 4% PFA and embedded in paraffin. Then 5 μm slices were prepared with a microtome (Leica, Germany), followed with deparaffinization, dehydration, and incubation in heat-mediated antigen retrieval sequentially. Subsequently, the endogenous catalase was eliminated with 3% H_2O_2-methanol, and tissue slices were incubated with the indicated primary antibodies against Ki67 (1:500, Servicebio, China, GB121141), CD31(1:500; abcam, ab182981) and F4/80 (1:2000, proteintech, China, 28463-1-AP) at 4°C overnight. After washing with PBS, sections were incubated with the biotinylated secondary antibodies at room temperature for 1 h, followed with incubation in peroxidase solution for 30 min staining with DAB reagent and counterstained with hematoxylin. The images of each section were captured and analyzed under optical microscope. The number of $ki67^+$, $CD31^+$ and $F4/80^+$ cells was counted using ImageJ and the plugin IHC Profiler.

In HE staining, the paraffin-embedded sections were sequentially deparaffinized, dehydrated, stained by hematoxylin, differentiated by the addition of hydrochloric ethanol, backed to blue with ammonia water, and stained with eosin. Then the sections were dehydrated with gradient alcohol, cleared with xylene, sealed with neutral resin, and observed under an optical microscope.

QUANTIFICATION AND STATISTICAL ANALYSIS

All statistical analysis were conducted with GraphPad Prism 9.0 (GraphPad Software, USA). Results were presented as means ± SD standard deviation on three independent experiments. Student's *t* test was performed to analyze the statistical difference between two groups, and analysis of variance (ANOVA) was applied to evaluate the differences between multiple groups. The p value <0.05 was considered statistically significant (*p < 0.05; **p < 0.01; ***p < 0.001; ****p < 0.0001). p-value >0.05 was considered not significant and was denoted by "ns".